sustainability

MDPI

Article

Stochastic Production Control of a Closed-Loop Hybrid Manufacturing–Remanufacturing System Considering Greenhouse Gas Emissions

Morad Assid [1], Ali Gharbi [1,*], Jean-Pierre Kenné [2] and Armel Leonel Kuegoua Takengny [2]

[1] Production System Design and Control Laboratory, Systems Engineering Department, École de Technologie Supérieure, University of Quebec, 1100 Notre-Dame West, Montreal, QC H3C 1K3, Canada; morad.assid@etsmtl.ca

[2] Production System Design and Control Laboratory, Mechanical Engineering Department, École de Technologie Supérieure, University of Quebec, 1100 Notre-Dame West, Montreal, QC H3C 1K3, Canada; jean-pierre.kenne@etsmtl.ca (J.-P.K.); armel-leonel.kuegoua-takengny.1@ens.etsmtl.ca (A.L.K.T.)

* Correspondence: ali.gharbi@etsmtl.ca; Tel.: +1-514-396-7574

Abstract

This paper addresses the stochastic optimal control of a closed-loop hybrid manufacturing–remanufacturing system (HMRS) operating under random machine failures and greenhouse gas (GHG) emission constraints in the context of sustainable industrial operations. The system consists of two dedicated machines for manufacturing and remanufacturing that jointly produce a single product in a dynamic production environment. The objective is to minimize the long-run expected total cost, including inventory holding and shortage costs, manufacturing and remanufacturing costs, and penalties associated with emissions exceeding a prescribed limit. The structure of the optimal production control policy is determined using a stochastic optimal control framework based on Hamilton–Jacobi–Bellman equations, whose optimality conditions are solved numerically. A sensitivity analysis is then conducted to examine the behavior of the resulting control policy under variations in key system parameters. The results show how coordinated manufacturing and remanufacturing decisions can be regulated through emission- and inventory-dependent thresholds in failure-prone hybrid production systems. This work contributes to the literature on sustainable manufacturing by providing a rigorous modeling and control framework for environmentally regulated hybrid manufacturing–remanufacturing systems.

Keywords: hybrid manufacturing–remanufacturing systems; stochastic process; production planning; closed-loop; GHG emissions

Academic Editor: Davide Settembre-Blundo

Received: 31 January 2026
Revised: 11 March 2026
Accepted: 13 March 2026
Published: 16 March 2026

1. Introduction

The growing emphasis on sustainable industrial practices has increased the need for manufacturing firms to adopt production strategies that reconcile economic performance, operational reliability, and environmental responsibility. In many industrial sectors, reducing greenhouse gas (GHG) emissions while ensuring production continuity has become a major challenge, particularly in environments subject to increasing regulatory pressure and operational uncertainty [1]. Governments and regulatory agencies worldwide have introduced emission caps, carbon taxes, and reporting requirements to limit the environmental footprint of manufacturing activities, while firms are simultaneously expected to maintain efficiency and service levels in uncertain operating environments [2–5]. Within

this context, sustainability has also become a key dimension of the Industry 4.0 paradigm, where production systems are increasingly supported by advanced monitoring and information infrastructures that enable the integration of environmental indicators into operational decisions.

Reverse logistics has emerged as a key enabler of sustainable and circular production systems by supporting the recovery, reuse, and reintegration of end-of-life products into manufacturing processes [6]. In this regard, hybrid manufacturing–remanufacturing systems (HMRSs), operating within closed-loop supply chains, combine conventional manufacturing with remanufacturing activities to restore returned products to a condition comparable to new items [7]. By reducing the consumption of virgin materials and limiting energy use, such systems contribute to environmental sustainability while also providing economic benefits. However, realizing these benefits requires coordinated planning and control of manufacturing and remanufacturing activities under both operational uncertainty and environmental regulation.

Planning and controlling HMRSs is particularly challenging because of the strong interdependence between manufacturing and remanufacturing operations, inventory dynamics, and system availability. In industrial environments, production capacity is affected by random machine failures and repairs, leading to stochastic fluctuations in available processing resources. At the same time, manufacturing and remanufacturing decisions jointly influence the accumulation of GHG emissions over time, introducing an additional dynamic state that directly impacts operational costs and admissible control actions [8]. Ignoring the combined effects of equipment unreliability and emission accumulation may lead to production strategies that are environmentally inefficient or economically fragile, thereby compromising the long-term sustainability of hybrid systems.

This work addresses this challenge by developing an integrated stochastic control framework for a closed-loop hybrid manufacturing–remanufacturing system operating under random machine failures and explicit GHG emission constraints. The central research problem concerns how manufacturing and remanufacturing rates should be jointly regulated over an infinite planning horizon in response to inventory levels, stochastic system availability, and cumulative emissions. The study seeks to address the following key questions: (i) how can manufacturing and remanufacturing activities be optimally coordinated to balance inventory-related costs and emission penalties under stochastic capacity variations? (ii) how does the accumulation of GHG emissions influence the structure and thresholds of optimal production policies? (iii) how sensitive is the structure of the optimal control policy to variations in key operational and environmental parameters? To address these questions, an optimal control policy is developed that jointly governs manufacturing and remanufacturing decisions in an unreliable closed-loop production system. The objective is to minimize the long-run expected total cost, including inventory holding and shortage costs, manufacturing and remanufacturing costs, and penalties associated with exceeding prescribed emission limits. The proposed model explicitly captures the joint dynamics of inventory evolution, machine availability, and cumulative GHG emissions within an infinite-horizon stochastic framework. The problem is formulated using stochastic optimal control theory and solved via dynamic programming, allowing the structure of the optimal integrated control policy to be characterized.

This research contributes to the literature on sustainable production management by extending stochastic optimal control approaches to environmentally constrained HMRSs with unreliable resources. By embedding emission considerations directly into production control decisions, the proposed framework provides decision-makers with analytical tools to manage operational uncertainty while ensuring compliance with environmental regulations. The remainder of this paper is organized as follows. Section 2 reviews the

relevant literature related to HMRSs and production planning and control (PPC) under GHG emission constraints. Section 3 describes the considered system and formulates the stochastic optimal control problem. Section 4 presents the optimality conditions and the numerical solution approach. Section 5 illustrates the proposed framework through a numerical example and analyzes the obtained results. Section 6 is devoted to sensitivity analyses aimed at validating the structure of the proposed control policy, while Section 7 discusses the managerial implications of the findings. Finally, Section 8 concludes the paper and outlines directions for future research.

2. Literature Review

The literature on PPC has extensively examined manufacturing and remanufacturing systems from economic, operational, and environmental perspectives. Contemporary industrial environments are increasingly characterized by operational complexity, notably due to frequent equipment failures and variability in repair durations, which are among the most disruptive factors affecting production processes [9]. Within this broad domain, HMRSs have attracted increasing attention because they support circular production by combining forward production and recovery operations [10,11]. Existing contributions can be broadly organized according to whether GHG emissions are explicitly incorporated into the decision-making process and whether equipment is assumed to be reliable or subject to random failures and repairs. A summary of the literature relevant to this study is presented in Table 1.

A substantial body of research addresses HMRSs without explicitly considering GHG emission control. These works primarily address economic objectives such as cost minimization, inventory coordination, production and remanufacturing decisions, and pricing strategies. In settings where equipment availability is assumed reliable, many studies adopt batch and order-based modeling perspectives to derive production and inventory policies under predictable capacity conditions. Classical contributions have examined inventory control structures and return acceptance or disposal decisions in hybrid systems [12–14]. More recent work has expanded the scope toward coordination mechanisms and planning structures in closed-loop contexts, including cyclic planning approaches that reduce setup and holding costs [15], and dynamic production planning under uncertain returns [16]. While this stream provides foundational insights into economic coordination in HMRSs, it typically assumes that production capacity is not disrupted by random breakdowns, which limits its ability to inform control decisions in failure-prone environments.

Other contributions extend HMRS analysis by explicitly modeling machine failures and repairs, thereby capturing the stochastic nature of effective production capacity. In such settings, continuous-time production control formulations are often attractive because they represent inventory evolution and capacity availability as dynamic state processes that can be adjusted through feedback decisions. A central policy paradigm in failure-prone production control is the Hedging Point Policy (HPP), originally introduced by Akella and Kumar [17]. Under the HPP, the production rate is regulated as a function of the system operational state and the inventory level, with the objective of building and maintaining safety stock during up periods to buffer expected capacity losses during downtime. In hybrid contexts, several studies have adapted such feedback ideas to coordinate manufacturing and remanufacturing decisions under disruptions. For example, Korugan et al. [18] investigated the impact of quality variability and return characteristics on the performance of HMRSs by modeling machine operations as continuous-time Markov chains and analyzing their effect on effective throughput, and Turki et al. [19] considered hedging-type control in closed-loop settings with failures. Recent advancements have incorporated machine learning techniques to support decision-making in flexible circular production environments [20],

and opportunistic-preventive maintenance strategies have been introduced to enhance overall system performance in deteriorating HMRSs [21]. Although this stream captures machine unreliability, most contributions focus primarily on economic performance and do not incorporate explicit GHG emission regulation, which limits the assessment of the cost-emission tradeoffs under stochastic capacity losses.

Motivated by regulatory pressure and voluntary sustainability initiatives, a growing body of research integrates GHG emission considerations into production planning models for HMRSs and closed-loop systems. In this class, environmental requirements such as carbon taxes, cap-and-trade schemes, or emission caps are incorporated into planning models, while machine unavailability is often not explicitly modeled. For instance, Bazan et al. [22] introduced a closed-loop supply chain model for remanufacturing under carbon tax penalties, and Wang and Han [23] analyzed joint procurement and production decisions under policy incentives such as subsidies and penalties in hybrid settings. Shekarian et al. [24] investigated dual-channel closed-loop supply chains with GHG-related objectives, highlighting the role of competition and channel structure in shaping forward and reverse decisions. In addition, Jauhari et al. [25] developed a closed-loop inventory model where manufacturing and remanufacturing operate simultaneously within a hybrid production system and emissions from multiple activities are regulated via a carbon tax; their results show that coordinating production allocation and collection-related decisions can reduce costs and emissions, while take-back incentives may increase returns but can also increase total emissions if not carefully managed. More recently, Lahmar et al. [26] proposed a multi-objective sustainable planning model for a hybrid multi-stage manufacturing–remanufacturing system that simultaneously minimizes total costs and CO_2 emissions while accounting for grade-based classifications of recovered and remanufactured products. Overall, despite their environmental relevance, these studies generally do not represent the operational consequences of random failures and repairs, which can materially change both production feasibility and the temporal profile of emissions.

Building on these streams, a smaller body of work considers environmentally constrained planning under equipment unreliability, but this literature remains fragmented in terms of system scope and policy characterization. Several contributions propose environmentally aware feedback policies that regulate production in response to emission-related thresholds in failure-prone settings, often motivated by carbon tax regulation [27]. However, many of these models are developed for manufacturing-only systems and do not explicitly capture the coupled dynamics of manufacturing and remanufacturing decisions. Recent HMRS-focused studies move in this direction but typically rely on integrated planning formulations rather than deriving an optimal feedback control structure. For example, Ndhaief et al. [28] incorporated environmental considerations into their analysis in order to reconcile economic performance with environmental compliance in a failure-prone hybrid manufacturing–remanufacturing system that relies on subcontracting. Their objective was to limit carbon emission overruns while maintaining a high level of demand satisfaction. Merghem et al. [29] investigated integrated production, maintenance, and quality planning in an imperfect HMRS with outsourcing opportunities and carbon emissions, accounting for deterioration and variability in return quality while assessing the combined impact of emissions and outsourcing on planning decisions. In a related HMRS leasing context, Liu et al. [30] modeled joint production and preventive maintenance decisions while explicitly accounting for carbon emission costs and uncertain quality that affects remanufacturing cost and equipment degradation; they used metaheuristic optimization to identify production quantities, maintenance periodicities, and remanufacturing cost thresholds that balance profit and emission reductions. Despite these advances, the literature still lacks a

unified stochastic optimal control treatment that endogenously derives the structure of an optimal feedback policy for failure-prone HMRSs under explicit GHG emission regulations.

Overall, the literature indicates that HMRSs have been widely studied either from an economic coordination perspective under reliable capacity assumptions or from a disruption-focused perspective that neglects explicit emission regulation. In parallel, environmentally constrained production planning has progressed substantially, but studies that jointly address manufacturing, remanufacturing, stochastic machine unavailability, and emission regulation remain limited, and many proposed control structures are either simplified planning formulations or policies calibrated a priori rather than derived endogenously from a unified stochastic optimal control framework. This gap is particularly critical because, under random failures and repairs, both inventory dynamics and emission accumulation can deviate substantially from nominal trajectories, so policies that ignore these interactions may lead to biased cost assessments and suboptimal operational responses. To address these limitations, the present work develops an integrated stochastic optimal control framework for a closed-loop HMRS subject to random failures and an explicit GHG constraint with penalty. The proposed approach goes beyond incremental adaptations of hedging-type policies by deriving a policy structure from dynamic programming and the associated optimality conditions, thereby providing a rigorous and implementable decision-support tool for coordinating manufacturing and remanufacturing activities while balancing long-run economic performance and environmental compliance.

Table 1. Relevant literature of models for HMRS with and without considering environmental aspects.

Research	Dedicated Facilities for Manufacturing and Remanufacturing	Failure-Prone Production Machines	Continuous Process Production	Environmental Approach	Developed New Production Control Policy
Class I. Models for HMRSs without GHG emission control					
Van Der Laan et al. [12]	×				
Dobos [13]	×		×		×
Gayon et al. [14]	×		×		
Aminipour et al. [15]					
Cheng [16]	×				
Korugan et al. [18]		×	×		
Turki et al. [19]	×	×	×		
Koulinas et al. [20]		×			
Assid et al. [21]		×	×		×
Class II. Models for HMRSs with GHG emission control					
Bazan et al. [22]	×			×	
Wang and Han [23]	×			×	
Shekarian et al. [24]				×	
Jauhari et al. [25]				×	
Lahmar et al. [26]				×	
Ndhaief et al. [28]	×	×	×	×	
Liu et al. [30]		×		×	
Merghem et al. [29]	×	×		×	
This Paper	×	×	×	×	×

3. System Description and Problem Formulation

For clarity and readability, the main notation used throughout the paper is summarized in Table 2.

Table 2. Summary of main notations.

Notation	Description
$x(t)$	inventory level of finished products at time t
$e(t)$	cumulative greenhouse gas (GHG) emission level of the system at time t
θ_1, θ_2	emission indices of the manufacturing and remanufacturing machines, respectively (emission volume per unit of product)
$u_1(t), u_2(t)$	production rates of the manufacturing and remanufacturing machines at time t
d	customer demand rate
$q_{\alpha\beta}$	transition rate from system mode α to mode β
$\xi(t)$	stochastic process describing the operational mode of the hybrid system at time t
ρ	discount rate
c^+	unit inventory cost
c^-	unit shortage cost
c_M	unit manufacturing cost
c_R	unit remanufacturing cost
c^e	unit penalty cost for GHG emissions exceeding the regulatory limit
L	prescribed GHG emission limit imposed by regulation
$g(\cdot)$	instantaneous cost function
$J(\cdot)$	expected total discounted cost over an infinite planning horizon
$v(\cdot)$	value function associated with the stochastic optimal control problem

The production system considered in this study is a closed-loop HMRS composed of two dedicated machines operating in parallel. The first machine, denoted by M_1, performs manufacturing operations using virgin raw materials, while the second machine, denoted by M_2, is dedicated to the remanufacturing of end-of-life products collected from the market. Both machines are subject to random breakdowns and repairs and produce a single type of finished product at time-dependent rates $u_1(t)$ and $u_2(t)$, respectively.

As illustrated in Figure 1, finished products are stored in an inventory with level $x(t)$ to satisfy customer demand. Manufacturing and remanufacturing activities generate GHG emissions during production, which accumulate over time and are represented by the state variable $e(t)$. The emission intensities associated with machines M_1 and M_2 are characterized by the coefficients θ_1 and θ_2, respectively. The system is equipped with an emission monitoring mechanism that measures cumulative emissions in equivalent units of CO_2. Under an emissions cap regulation, an environmental penalty is incurred whenever the cumulative emission level exceeds the prescribed limit L. The formulation of the problem relies on the following assumptions:

- Virgin raw materials and returned products are assumed to be sufficiently available to supply the manufacturing and remanufacturing processes;
- Remanufactured products are assumed to be equivalent in quality to newly manufactured products and are fully substitutable in satisfying demand;
- Customer demand rate is assumed to be constant and known;
- Customer demand is satisfied by the combined output of both production machines.

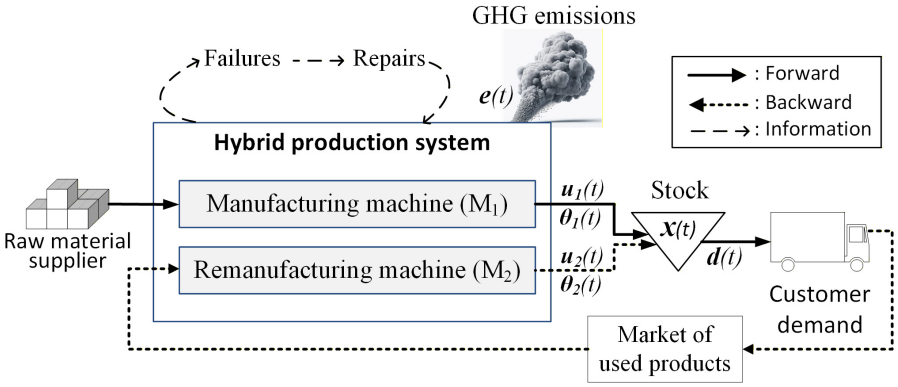

Figure 1. Structure of the hybrid manufacturing–remanufacturing system.

To capture the stochastic nature of machine availability, the operational state of each machine is modeled explicitly. Let $\{\xi_m(t), t \geq 0\}$ be the stochastic process describing the state of machine m ($m = 1,2$), where $\xi_m(t)$ takes values in the finite set $\Omega_m = \{1,2\}$, corresponding to the operational and failed states, respectively.

The overall system state at time t is described by the process $\xi(t) = (\xi_1(t), \xi_2(t))$. Consequently, the HMRS can be represented as a continuous-time stochastic process with a hybrid state, where $\xi(t)$ evolves according to a non-homogeneous semi-Markov process with a finite state space $\Omega = \{1,2,3,4\}$, as summarized in Table 3.

Table 3. Operational modes of the manufacturing and remanufacturing machines in the HMRS.

$\xi_1(t)$	1	1	2	2
$\xi_2(t)$	1	2	1	2
$\xi(t)$	1	2	3	4

The stochastic evolution of the system modes is governed by transition probabilities between operational states. For a sufficiently small time increment δt, the transition probabilities of the process $\xi(t)$ are defined as:

$$\mathbb{P}\{\xi(t+\delta t) = \beta \mid \xi(t) = \alpha\} = \begin{cases} q_{\alpha\beta}\,\delta t + o(\delta t), & \text{if } \alpha \neq \beta, \\ 1 + q_{\alpha\alpha}\,\delta t + o(\delta t), & \text{if } \alpha = \beta, \end{cases} \tag{1}$$

where $q_{\alpha\beta}$ denotes the transition rate from mode α to mode β, with $q_{\alpha\beta} \geq 0$ for $\alpha \neq \beta$, and

$$q_{\alpha\alpha} = -\sum_{\beta \neq \alpha} q_{\alpha\beta}. \tag{2}$$

The term $o(\delta t)$ satisfies $\lim_{\delta t \to 0} \frac{o(\delta t)}{\delta t} = 0$.

The hybrid system can randomly switch between four operational modes depending on the failure and repair states of the manufacturing and remanufacturing machines. These transitions explicitly represent breakdown and repair events for each machine and are summarized in the state transition diagram shown in Figure 2, where the transition rates correspond to failure and repair intensities between modes.

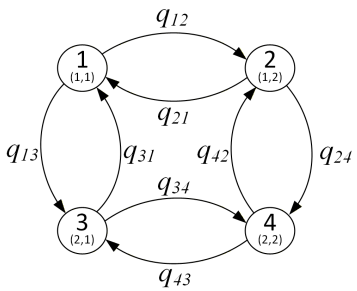

Figure 2. State transition diagram of the stochastic process.

Over an infinite planning horizon, the system may randomly switch between the different operational modes. The stochastic process $\xi(t)$ is therefore characterized by a continuous-time Markov chain with a 4×4 transition rate matrix $Q = [q_{\alpha\beta}]$, defined as:

$$Q = \begin{pmatrix} q_{11} & q_{12} & q_{13} & 0 \\ q_{21} & q_{22} & 0 & q_{24} \\ q_{31} & 0 & q_{33} & q_{34} \\ 0 & q_{42} & q_{43} & q_{44} \end{pmatrix}. \tag{3}$$

The feasibility condition ensuring that the long-run average production capacity exceeds demand is expressed as:

$$\pi_1(u_{1max} + u_{2max}) + \pi_2 \cdot u_{1max} + \pi_3 \cdot u_{2max} \geq d \tag{4}$$

with π_i, $i = 1, 2, 3, 4$ denote the steady-state probabilities associated with system mode i. These probabilities are obtained by solving the Kolmogorov forward equations:

$$\pi \cdot Q = 0 \tag{5}$$

$$\sum_{i=1}^{4} \pi_i = 1. \tag{6}$$

The dynamics of the finished product inventory are described by the following differential equation:

$$\dot{x}(t) = u_1(t) + u_2(t) - d \tag{7}$$

with initial condition $x(0) = x_0$. The terms $u_1(t)$ and $u_2(t)$ denote the production rates of machines M_1 and M_2, respectively, while d represents the demand rate. A positive value of $x(t)$ indicates the presence of finished products in inventory, whereas a negative value corresponds to a shortage situation.

Following the modeling approach proposed in [27], the evolution of the cumulative emission level is assumed to be directly linked to the production activities of the system. The emission level $e(t)$ at time t evolves according to the differential equation:

$$\dot{e}(t) = \theta_1 \cdot u_1(t) + \theta_2 \cdot u_2(t) \tag{8}$$

with initial condition $e(0) = e_0$. The parameters θ_1 and θ_2 denote the emission indices associated with manufacturing and remanufacturing operations, respectively, expressed in units of emission per unit of finished product. The emission level is assumed to be continuous over time, including at repair completion instants, so that $e(T^+) = e(T^-)$.

The admissible control domain defines the feasibility plan for the decision variables. As in Equation (9), such a domain depends on the stochastic process $\xi(t)$ and is given by:

$$\Gamma(\xi) = \left\{ \begin{array}{l} (u_1(t), u_2(t)) \in \mathbb{R}^2 \\ 0 \leq u_1(t) \leq u_{1max} \cdot \text{Ind}\{\xi = 1, 2\} \\ 0 \leq u_2(t) \leq u_{2max} \cdot \text{Ind}\{\xi = 1, 3\} \end{array} \right\}. \tag{9}$$

The notation $\text{Ind}\{\delta(\cdot)\}$ denotes the indicator function of the condition $\delta(\cdot)$, defined as:

$$\text{Ind}\{\delta(\cdot)\} = \left\{ \begin{array}{l} 1 \text{ if } \delta(\cdot) \text{ is true,} \\ 2 \text{ if not.} \end{array} \right. \tag{10}$$

The instantaneous cost function $g(\cdot)$, defined in Equation (11), accounts for inventory holding and shortage costs, manufacturing and remanufacturing production costs, as well as the penalty associated with GHG emissions.

$$g(x, u_1, u_2, e) = c^+ \cdot x^+ + c^- \cdot x^- + c(u_1, u_2) + c_e(e). \tag{11}$$

Inventory holding and shortage costs are used to penalize deviations of the finished product inventory from zero. Let c^+ and c^- denote the unit holding and shortage cost rates, respectively. These costs are defined using the functions $x^+ = \max(0, x)$ and $x^- = \max(0, -x)$. Production costs in the hybrid system are assumed to be linear with respect to the production rates and are represented by the function $c(u_1, u_2)$, defined as follows:

$$\begin{array}{r} c(u_1, u_2) = (c_M u_1 + c_R u_2) \cdot \text{Ind}\{\xi(t) = 1\} + c_M u_1 \cdot \text{Ind}\{\xi(t) = 2\} + c_R u_2 \\ \cdot \text{Ind}\{\xi(t) = 3\} \end{array} \tag{12}$$

where c_M and c_R denote the unit production costs associated with manufacturing and remanufacturing, respectively.

Under an emissions cap regulation, when the cumulative emission level exceeds the prescribed limit L imposed by regulatory authorities, the excess emissions are penalized through an environmental cost, following the approach proposed by [27]. The corresponding penalty cost is defined as:

$$c_e(e) = c^e \cdot max\{0, (e(t) - L)\} \tag{13}$$

where c^e denotes the unit penalty cost associated with emissions exceeding the limit L, expressed in monetary units per unit of emission volume.

The objective is to determine the control variables, namely the manufacturing and remanufacturing production rates $u_1(\cdot)$ and $u_2(\cdot)$, that minimize the expected total discounted cost $J(\cdot)$, defined as:

$$J(x, e, u_1, u_2, \alpha) = E\left\{ \int_0^\infty e^{-\rho t} g(x, u_1, u_2, e) dt \mid x(0) = x, \xi(0) = \alpha \right\} \tag{14}$$

where ρ denotes the discount rate. The variables x and α represent the initial values of the inventory level and the system mode, respectively.

The value function associated with this optimization problem is defined as:

$$v(e, x, \alpha) = \min_{(u_1, u_2) \in \Gamma(\alpha)} J(x, e, u_1, u_2, \alpha). \tag{15}$$

The optimality conditions that the value function defined in Equation (15) must satisfy are presented in the next section.

4. Optimality Conditions and Numerical Methods

The value function $v(e, x, \alpha)$, defined as the minimum expected discounted cost starting from state (e, x, α), satisfies a system of coupled Hamilton–Jacobi–Bellman (HJB) equations derived using a stochastic dynamic programming framework. These equations characterize the optimal trade-off between production, inventory, and emission-related costs while accounting for stochastic machine availability.

For each system mode $\alpha \in \Omega$, the HJB equations take the following form:

$$\begin{aligned} \rho v(x, e, \alpha) = \min_{(u_1, u_2) \in \Gamma(\alpha)} \Big[& g(\cdot) + \tfrac{\partial v(\cdot)}{\partial x}(u_1 + u_2 - d) + \tfrac{\partial v(\cdot)}{\partial e}(\theta_1 u_1 + \theta_2 u_2). \\ & + \sum_{\beta \in \Omega} q_{\alpha\beta} v(x, \varphi_e(\beta), \beta) \Big] \end{aligned} \tag{16}$$

where $\alpha \in \Omega$ denotes the current system mode, and $\varphi_e(\beta)$ represents the possible discontinuity of the emission state induced by a transition of the Markov process $\xi(t)$.

The function $\varphi_e(\cdot)$ describes the evolution of the emission level at jump times τ of the process $\xi(t)$ and is defined as follows:

$$\varphi_e(\xi) = \begin{cases} e(\tau^+) \text{ if } \begin{cases} \xi(\tau^+) = 1 \ \ and \ \ \xi(\tau^-) = 2, \\ \xi(\tau^+) = 1 \ \ and \ \ \xi(\tau^-) = 3, \end{cases} \\ e(\tau^-) \text{ otherwise.} \end{cases} \tag{17}$$

This formulation reflects the fact that emission accumulation is reset only under specific transitions of machine availability, while remaining continuous in all other cases.

The HJB equations defined in Equation (16) constitute a system of coupled partial differential equations for which closed-form solutions are available only in very specific and simplified settings, such as single-machine systems producing a single product [17]. For hybrid and failure-prone systems such as the one considered in this study, numerical solution techniques are therefore required, as recently used in [27,31]. In line with the policy iteration method proposed in [32], the HJB Equation (16) is solved numerically by approximating the value function $v(x, e, \alpha)$ with $v_h(x, e, \alpha)$ and by approximating its first-order partial derivatives $\partial v(x, e, \alpha)/\partial x$ and $\partial v(x, e, \alpha)/\partial e$ using finite-difference schemes. The continuous state variables x and e are discretized using uniform steps h_x and h_e, respectively. The value function is approximated by $v_h(x, e, \alpha)$ on this discrete grid. The numerical resolution of the discrete HJB system was implemented using MATLAB R2023b. The finite-difference discretization, policy iteration procedure, and convergence verification were coded in a structured algorithm that iteratively updates the value function until the maximum absolute difference between successive iterations falls below a prescribed tolerance level. This computational implementation allows reproducibility of the numerical results and ensures numerical stability of the solution process.

The first-order partial derivatives of the value function with respect to the inventory and emission states are approximated using finite-difference schemes to ensure numerical stability. The derivative with respect to the inventory level is given by:

$$\frac{\partial v(x, e, \alpha)}{\partial x} = \begin{cases} \frac{v_h(x + h_x, e, \alpha) - v_h(x, e, \alpha)}{h_x} \text{ if } u_1 + u_2 - d \geq 0\,, \\ \frac{v_h(x, e, \alpha) - v_h(x - h_x, e, \alpha)}{h_x} \text{ if } u_1 + u_2 - d < 0\,, \end{cases} \tag{18}$$

while the derivative with respect to the emission level is approximated by:

$$\frac{\partial v(x,e,\alpha)}{\partial e} = \frac{v_h(x,e+h_e,\alpha) - v_h(x,e,\alpha)}{h_e}. \tag{19}$$

By substituting the finite-difference approximations Equations (18) and (19) into Equation (16) and rearranging terms, the following system of discrete HJB equations is obtained for each mode $\alpha \in \Omega = \{1,2,3,4\}$:

$$\begin{aligned} &v_h(x,e,1) \\ &= \min_{(u_1,u_2)\in\Gamma(1)} \left[\frac{1}{\left(\rho + \frac{|u_1+u_2-d|}{h_x} + \frac{(\theta_1 u_1+\theta_2 u_2)}{h_e} - q_{11} \right)} \cdot \left[\begin{array}{l} g(x,e,1) \\ + \frac{|u_1+u_2-d|}{h_x} \left(\begin{array}{l} v_h(x+h_x,e,1) I_1^+ \\ + v_h(x-h_x,e,1) I_1^- \end{array} \right) \\ + \frac{(\theta_1 u_1+\theta_2 u_2)}{h_e} v_h(x,e+h_e,1) \\ + q_{12} v_h(x,\varphi_e(2),2) + q_{13} v_h(x,\varphi_e(3),3) \end{array} \right] \right], \end{aligned} \tag{20}$$

$$\begin{aligned} &v_h(x,e,2) \\ &= \min_{u_1\in\Gamma(2)} \left[\frac{1}{\left(\rho + \frac{|u_1-d|}{h_x} + \frac{\theta_1 u_1}{h_e} - q_{22} \right)} \cdot \left[\begin{array}{l} g(x,e,2) \\ + \frac{|u_1-d|}{h_x} \left(\begin{array}{l} v_h(x+h_x,e,2) I_2^+ \\ + v_h(x-h_x,e,2) I_2^- \end{array} \right) \\ + \frac{\theta_1 u_1}{h_e} v_h(x,e+h_e,2) \\ + q_{21} v_h(x,\varphi_e(1),1) + q_{24} v_h(x,\varphi_e(4),4) \end{array} \right] \right], \end{aligned} \tag{21}$$

$$\begin{aligned} &v_h(x,e,3) \\ &= \min_{u_2\in\Gamma(3)} \left[\frac{1}{\left(\rho + \frac{|u_2-d|}{h_x} + \frac{\theta_2 u_2}{h_e} - q_{33} \right)} \cdot \left[\begin{array}{l} g(x,e,3) \\ + \frac{|u_2-d|}{h_x} \left(\begin{array}{l} v_h(x+h_x,e,2) I_3^+ \\ + v_h(x-h_x,e,3) I_3^- \end{array} \right) \\ + \frac{\theta_2 u_2}{h_e} v_h(x,e+h_e,3) \\ + q_{31} v_h(x,\varphi_e(1),1) + q_{34} v_h(x,\varphi_e(4),4) \end{array} \right] \right], \end{aligned} \tag{22}$$

$$v_h(x,e,4) = \frac{1}{\left(\rho + \frac{d}{h_x} - q_{44} \right)} \cdot \left[\begin{array}{l} g(x,e,4) \\ + \frac{d}{h_x} v_h(x-h_x,e,4) \\ + q_{42} v_h(x,\varphi_e(2),2) \\ + q_{43} v_h(x,\varphi_e(3),3) \end{array} \right] \tag{23}$$

where I_1^+, I_1^-, I_2^+, I_2^-, I_3^+, and I_3^- denote indicator functions associated with the sign of the net production flow in each operating mode.

The numerical resolution of the discrete HJB equations makes it possible to determine the structure of the optimal production control policy. The next section presents a numerical example used to illustrate and analyze this structure.

5. Numerical Example and Results Analysis

This section provides a numerical example to illustrate the results obtained. The resolution domain is defined by:

$$D(x,e) = G_h(x) \cdot G_h(e)$$

where $G_h(x) = \{x : -5 \le x \le 70\}$ and $G_h(e) = \{e : 0 \le e \le 350\}$ with $h_x = 0.5$ and $h_e = 5$.

The parameter values used in the numerical example, reported in Table 4, are selected to be consistent with assumptions and empirical evidence commonly documented in the remanufacturing and closed-loop supply chain literature. In particular, the unit remanufacturing cost is assumed to be lower than the manufacturing cost ($c_R < c_M$), reflecting component reuse and reduced raw material consumption [33,34]. At the same time, the maximum remanufacturing rate is assumed to be lower than the manufacturing rate ($u_{2max} < u_{1max}$) due to the additional processing stages typically involved in remanufactur-

ing operations, which tend to increase operational complexity and processing time [35,36]. Regarding environmental parameters, the emission indices are selected to reflect different emission intensities between the two production modes, with remanufacturing assumed to generate higher emissions than manufacturing ($\theta_2 > \theta_1$). This choice reflects the fact that remanufacturing may require additional processing operations and energy use per unit, and is consistent with environmentally regulated production settings where mode-dependent emission factors are commonly considered [36,37]. Failure and repair rates are selected to ensure a realistic balance between operational availability and disruption frequency, consistent with stochastic production control studies. Overall, the parameter configuration is designed to satisfy the feasibility condition stated in Equation (4) while remaining consistent with structural relationships documented in the literature.

Table 4. Numerical example data.

c^+	c^-	c_M	c_R	c^e	u_{1max}	u_{2max}	d	L	θ_1	θ_2	q_{12}^1	q_{12}^2	q_{21}^1	q_{21}^2
5	200	150	50	60	3.5	3.25	3	250	1.5	3	0.01	0.0125	0.15	0.15

Although the numerical illustration is simulation-based, the parameter relationships and structural assumptions are calibrated to reflect documented industrial practices in remanufacturing sectors such as retreaded tires, cartridges, and heavy-duty and off-road equipment. In these industries, manufacturing and remanufacturing activities exhibit differentiated cost structures, capacity constraints, and environmental impacts, and emission generation represents a measurable operational concern [38,39]. The purpose of the numerical study is therefore not to replicate a specific company dataset, but to illustrate the structural behavior of the optimal emission-dependent control policy under realistic industrial configurations. The numerical resolution of the discretized HJB equations, implemented in MATLAB R2023b, provides a computational framework that can be applied to different parameter values and system configurations once the corresponding operational data are available. In this study, a single baseline configuration is presented to illustrate the structure of the optimal control policy, while the following sensitivity analysis (see Section 6) investigates how the policy structure evolves when key system parameters are varied.

The optimal production control policies obtained for the considered system are illustrated in Figures 3–5. These policies extend the concept of emission-sensitive threshold-based control to a hybrid manufacturing–remanufacturing context with reverse logistics. The figures depict the production rates of the manufacturing and remanufacturing machines as functions of the finished product inventory level, reflecting the need to build adequate safety stock to hedge against random breakdowns and repairs while limiting penalty costs associated with emissions exceeding the prescribed limit L.

The optimal production control policies for the considered system are formally defined by Equations (24)–(27). These policies depend on the operational state of the machines and are characterized by a set of inventory-based critical thresholds that regulate production decisions under emission constraints.

When both the manufacturing machine M_1 and the remanufacturing machine M_2 are operational (mode 1), production decisions are governed by the control policies defined in Equations (24) and (25). In this mode, the manufacturing machine is regulated by two critical inventory thresholds. The threshold $Z_1(e)$ applies when the emission level remains below the regulatory limit L, whereas a fixed threshold Z_2 is used once the emission level exceeds this limit. In contrast, the remanufacturing machine is controlled by

a single emission-dependent inventory threshold $Z_3(e)$, which applies regardless of the emission regime.

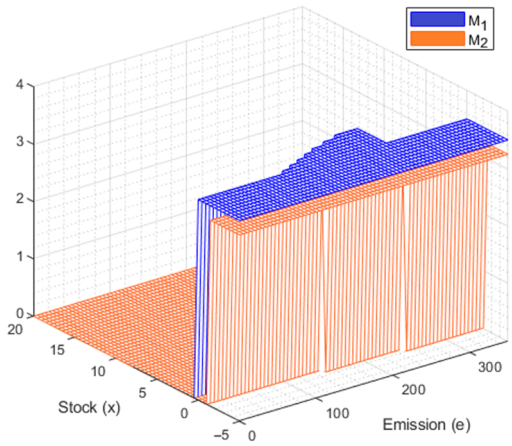

(**a**) Production rates of M_1 and M_2

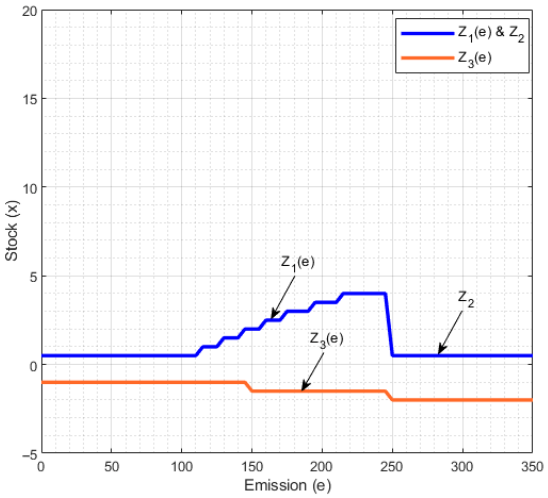

(**b**) Traces of production thresholds

Figure 3. Production rate when both machines are operational.

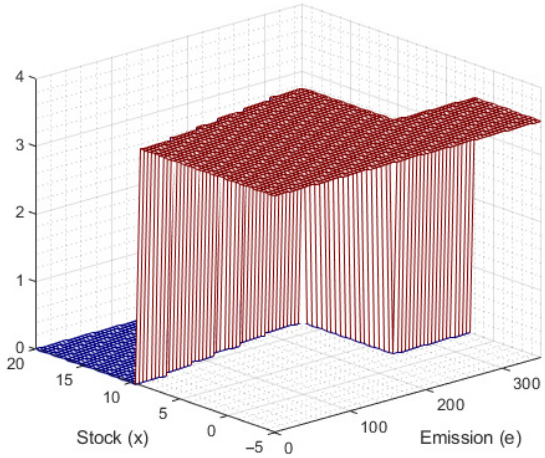

(**a**) Production rate of M_1

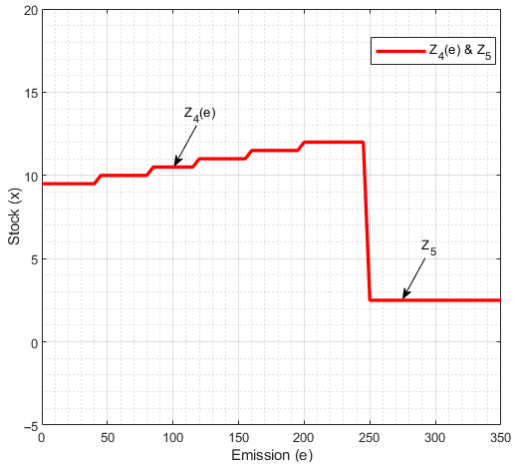

(**b**) Traces of production thresholds

Figure 4. Production rate when the manufacturing machine is operational.

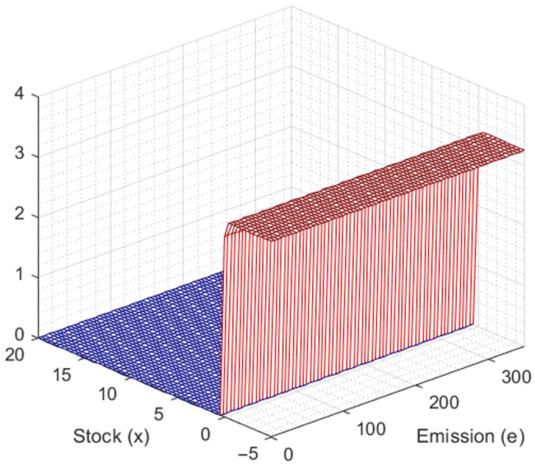

(**a**) Production rate of M_2

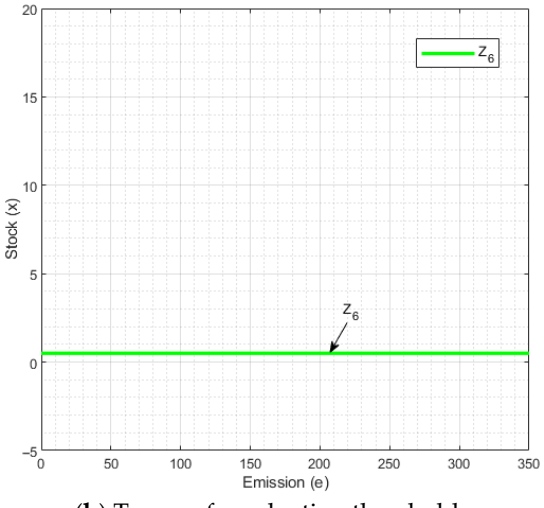

(**b**) Traces of production thresholds

Figure 5. Production rate when the remanufacturing machine is operational.

For the manufacturing machine, two emission regimes are therefore distinguished. When $e < L$, production decisions depend on the threshold $Z_1(e)$: the machine operates at its maximum rate when the inventory level is below this threshold, produces at the demand rate when the threshold is reached, and stops production otherwise. When $e \geq L$, a more restrictive threshold Z_2 applies, reflecting the need to limit additional emission accumulation and associated penalties. The same three-stage production logic is preserved, but production is curtailed at a lower inventory level.

For the remanufacturing machine, a single threshold-based rule applies. When the inventory level is below $Z_3(e)$, the machine produces at its maximum rate; it produces at the demand rate when the threshold is reached and stops production otherwise.

$$\begin{cases} \text{When } e < L: \\ \quad u_1(x,e,1) = \begin{cases} u_{1max} & \text{if } x < Z_1(e) \\ d & \text{if } x = Z_1(e) \\ 0 & \text{otherwise} \end{cases} \\ \text{When } e \geq L: \\ \quad u_1(x,e,1) = \begin{cases} u_{1max} & \text{if } x < Z_2 \\ d & \text{if } x = Z_2 \\ 0 & \text{otherwise} \end{cases} \end{cases} \tag{24}$$

$$u_2(x,e,1) = \begin{cases} u_{2max} & \text{if } x < Z_3(e) \\ d & \text{if } x = Z_3(e) \\ 0 & \text{othersize} \end{cases} \tag{25}$$

When the remanufacturing machine becomes unavailable due to a breakdown (mode 2), production is carried out exclusively by the manufacturing machine. The corresponding control policy is given by Equation (26), in which the manufacturing machine is regulated by two inventory thresholds depending on the emission level.

Specifically, when the emission level remains below the limit L, production decisions are governed by the emission-dependent threshold $Z_4(e)$. Once the emission level exceeds L, a more conservative threshold Z_5 applies. In both regimes, the manufacturing machine follows a three-stage production rule based on the inventory position relative to the corresponding threshold: production at the maximum rate below the threshold, production at the demand rate at the threshold, and no production otherwise.

$$\begin{cases} \text{When } e < L: \\ \quad u_1(x,e,2) = \begin{cases} u_{1max} & \text{if } x < Z_4(e) \\ d & \text{if } x = Z_4(e) \\ 0 & \text{otherwise} \end{cases} \\ \text{When } e \geq L: \\ \quad u_1(x,e,2) = \begin{cases} u_{1max} & \text{if } x < Z_5 \\ d & \text{if } x = Z_5 \\ 0 & \text{otherwise} \end{cases} \end{cases} \tag{26}$$

Conversely, when the manufacturing machine is unavailable (mode 3), production relies solely on the remanufacturing machine, and the control policy is defined by Equation (27). In this case, production decisions are governed by a single critical inventory threshold Z_6, which does not depend on the emission level.

The remanufacturing machine operates at its maximum rate when the inventory level is below Z_6, produces at the demand rate when the threshold is reached, and stops production otherwise.

$$u_2(x,e,3) = \begin{cases} u_{2max} & \text{if } x < Z_6 \\ d & \text{if } x = Z_6 \\ 0 & \text{otherwise} \end{cases} \quad (27)$$

The thresholds reported in the control laws (e.g., $Z_1(e)$, $Z_3(e)$, and $Z_4(e)$) are obtained directly from the numerical solution of the discretized HJB equations on the grid $(x,e) = G_h(x) \cdot G_h(e)$. Figures 3b, 4b and 5b show the switching traces of the policies presented in Figures 3a, 4a and 5a, which depict the optimal policies obtained from the numerical solution of the HJB equations. These traces illustrate the evolution of the critical thresholds as a function of emissions. For each emission grid point e_j, the optimal control is computed at all inventory nodes x_i and the switching point is identified as the inventory level at which the optimal action changes between the regimes "produce at u_{max}", "produce at d", and "stop". This procedure yields a discrete mapping $e_j \to Z_k(e_j)$ for each emission-dependent threshold $Z_k(\cdot)$. For practical reporting and implementation, this discrete mapping can be summarized using a segmented representation of the emission domain: the emission range is partitioned into a finite number of intervals $[E_k, E_{k+1})$, and a representative threshold value is assigned to each interval (e.g., the minimum or a central value of $Z_k(e_j)$ over the interval). This reduced representation preserves the policy structure observed on the full grid while providing a compact and reproducible description of how thresholds evolve with the emission level.

The structure of the obtained control policy reflects an explicit trade-off between inventory protection, emission accumulation, and stochastic capacity availability. The inventory thresholds act as safety buffers designed to protect the system against random machine failures and repair periods, thereby ensuring service continuity under uncertainty. Their dependence on the cumulative emission level captures the increasing marginal cost associated with continued production as emissions accumulate over time. When emissions remain below the regulatory limit, the policy tolerates higher safety stock levels in order to hedge against capacity losses. As emissions approach or exceed the prescribed limit, production decisions become more conservative, leading to lower admissible inventory thresholds that limit further emission accumulation and associated penalties. This interaction between inventory control and emission regulation explains the differentiated threshold structures observed across system modes and highlights the coordinated role of manufacturing and remanufacturing activities in achieving both operational reliability and environmental compliance.

The robustness of the proposed framework and the sensitivity of the critical thresholds with respect to key model parameters are further investigated through the sensitivity analyses presented in the next section.

6. Sensitivity Analysis

The robustness of the optimal manufacturing and remanufacturing control policies is evaluated through a sensitivity analysis that examines the impact of variations in selected model parameters. The analysis focuses on the behavior of the critical inventory thresholds $Z_i (i = 1,2,3)$ that characterize the control structure when both machines operate simultaneously. In particular, variations in economic parameters, including manufacturing, remanufacturing, and emission penalty costs, as well as key system parameters such as emission indices and maximum production rates, are considered. This analysis illustrates how the structure of the control policy responds to variations in parameter values within the proposed numerical framework. For clarity of presentation, the effects of these pa-

rameter changes are illustrated separately for the manufacturing machine M_1 and the remanufacturing machine M_2.

6.1. Manufacturing Cost

The results illustrated in Figure 6 correspond to three values of the manufacturing cost, $c_M = 50, 100, 150$. The results indicate that an increase in the manufacturing cost leads the system to reduce production at the maximum rate on the manufacturing machine M_1, while reallocating a larger share of production to the remanufacturing machine M_2. This shift is reflected in a decrease in the critical inventory threshold Z_1 associated with machine M_1, whereas the thresholds Z_2 and Z_3 remain unchanged. This behavior highlights that Z_2 and Z_3 are not directly affected by variations in the manufacturing cost. The observed results are consistent with the hybrid structure of the system, in which the remanufacturing machine acts as a complementary resource that can partially substitute manufacturing activities in order to preserve the economic viability of the system.

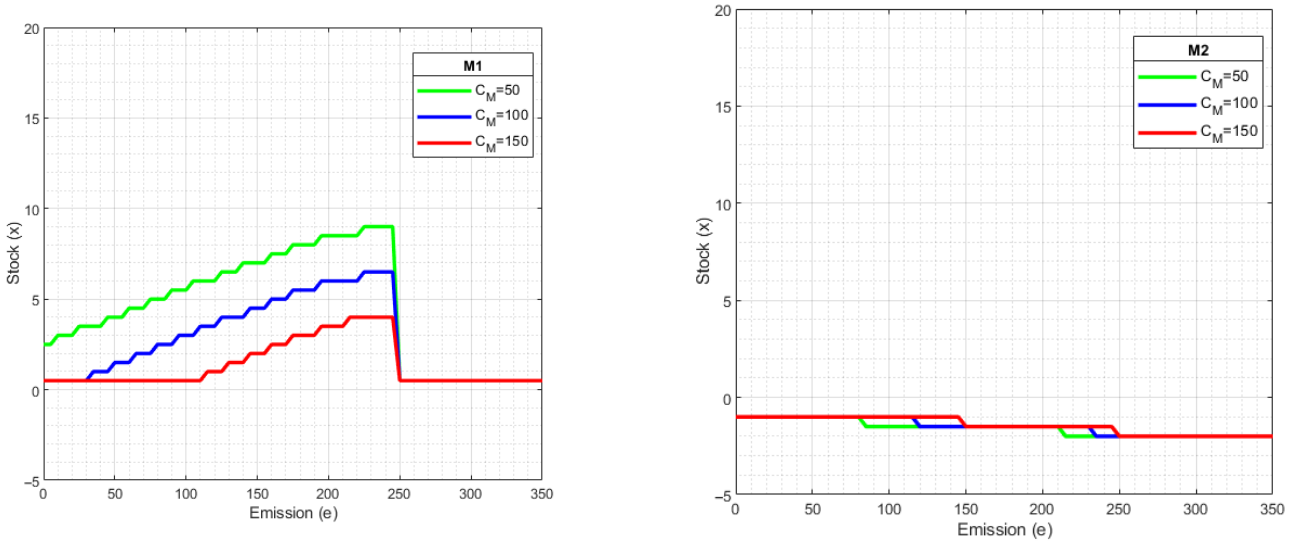

(**a**) Manufacturing machine (**b**) Remanufacturing machine

Figure 6. Variation in manufacturing costs and impact on critical thresholds.

6.2. Remanufacturing Cost

Figure 7 presents the sensitivity of the control policy with respect to three values of the remanufacturing cost, $c_R = 50, 100, 150$. An increase in c_R encourages the system to rely more heavily on the manufacturing machine M_1, which operates more frequently at its maximum rate, while production on the remanufacturing machine M_2 is reduced. This behavior results in an increase in the critical threshold Z_1 of the manufacturing machine and a decrease in the critical threshold Z_3 associated with the remanufacturing machine as the emission level increases. This outcome reflects the economic role of the manufacturing machine as a backup resource that compensates for higher remanufacturing costs, thereby ensuring that the hybrid system remains cost-effective and that prior investments are adequately recovered.

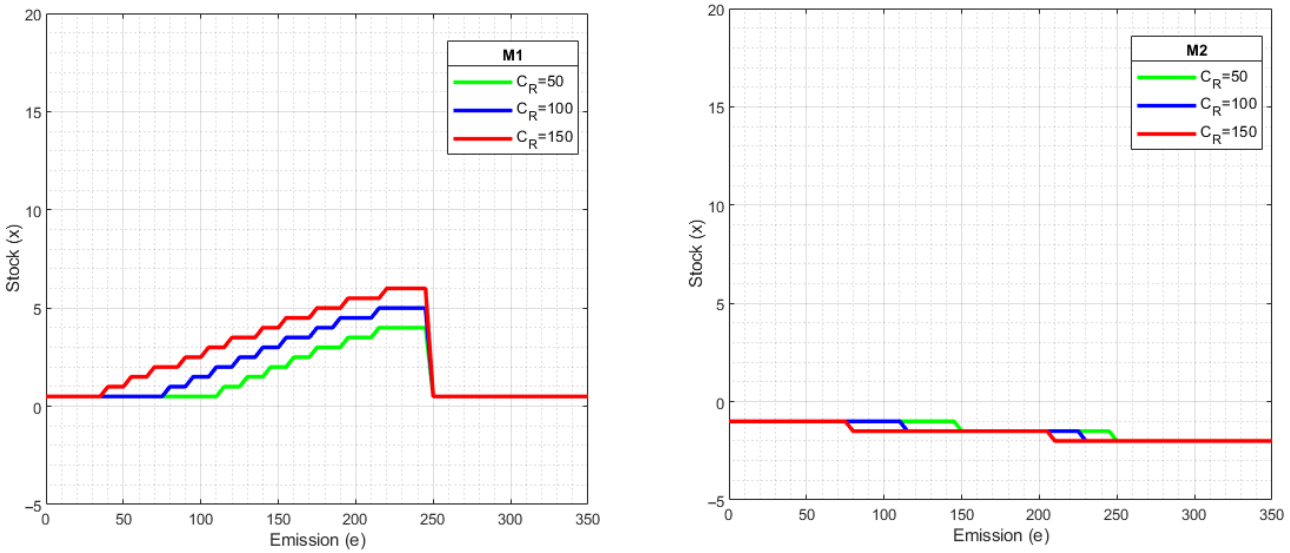

(**a**) Manufacturing machine (**b**) Remanufacturing machine

Figure 7. Variation in remanufacturing costs and impact on critical thresholds.

6.3. Emission Cost

The impact of the emission penalty cost is illustrated in Figure 8 for three values of $c^e = 40, 60, 80$. As the emission cost increases, the system tends to reduce production on the remanufacturing machine M_2, while increasing reliance on the manufacturing machine M_1. Consequently, the critical threshold Z_1 of the manufacturing machine increases, whereas the threshold Z_3 of the remanufacturing machine decreases with the emission level. This behavior is explained by the fact that the remanufacturing process is associated with a higher emission intensity ($\theta_2 > \theta_1$). As emission penalties increase, production on the more emission-intensive resource becomes less attractive, leading the system to favor the manufacturing machine despite its higher production cost.

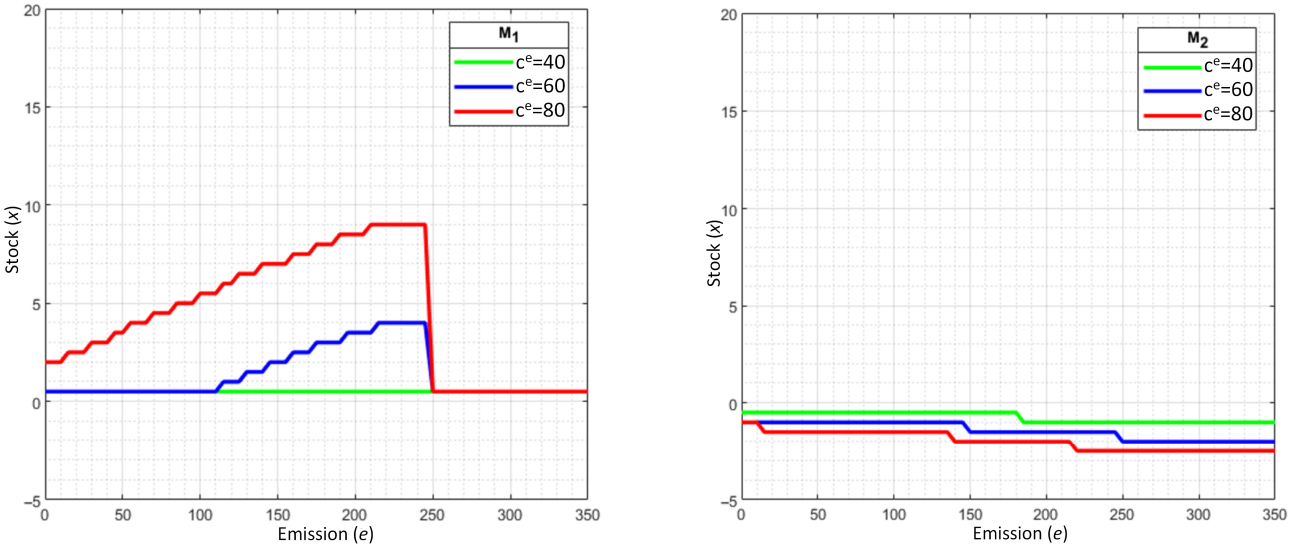

(**a**) Manufacturing machine (**b**) Remanufacturing machine

Figure 8. Variation in emission costs and impact on critical thresholds.

6.4. Manufacturing Machine Emission Index

Figure 9 illustrates the sensitivity of the control policy to variations in the emission index of the manufacturing machine, with $\theta_1 = 0.5, 1.5, 2.5$. An increase in θ_1, which im-

plies higher emissions per unit produced by M_1, leads the system to reduce manufacturing activity at the maximum rate and to increase production on the remanufacturing machine. This adjustment is associated with a decrease in the critical threshold Z_1 of the manufacturing machine and an increase in the threshold Z_3 of the remanufacturing machine as emissions accumulate. Such a response aims to limit excessive emission penalties once the emission limit L is approached or exceeded, while maintaining a balanced utilization of both machines within the hybrid system.

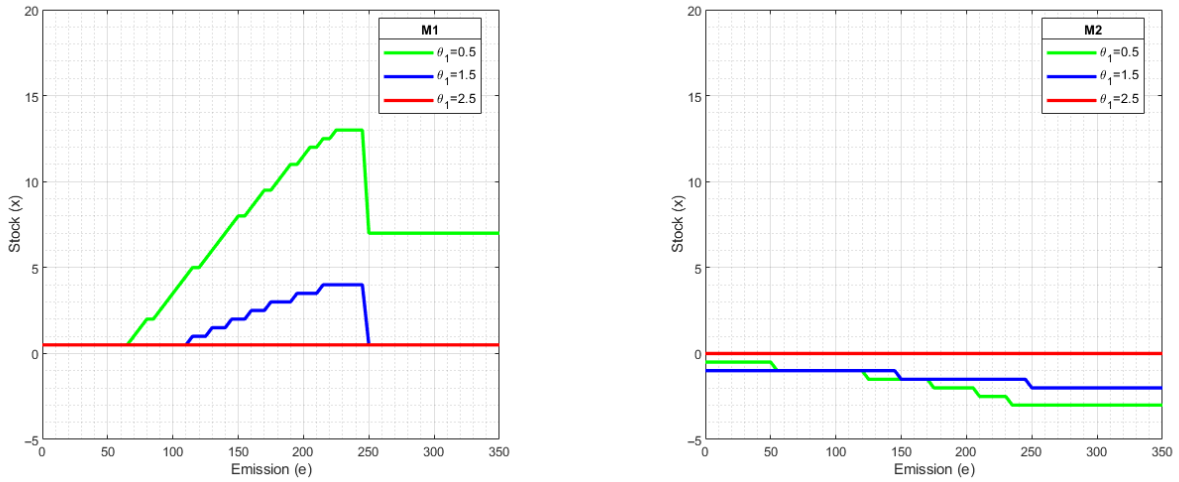

(**a**) Manufacturing machine (**b**) Remanufacturing machine

Figure 9. Variation in manufacturing machine emission index and impact on critical thresholds.

6.5. Remanufacturing Machine Emission Index

The sensitivity results presented in Figure 10 correspond to three values of the remanufacturing machine emission index, $\theta_2 = 2, 3, 4$. As θ_2 increases, indicating a more polluting remanufacturing process, the system shifts production toward the manufacturing machine M_1 and reduces reliance on M_2. This shift leads to an increase in the critical threshold Z_1 of the manufacturing machine and a decrease in the critical threshold Z_3 of the remanufacturing machine with the emission level. Such behavior allows the system to limit excessive emission penalties beyond the regulatory limit L while preserving the operational balance between manufacturing and remanufacturing activities.

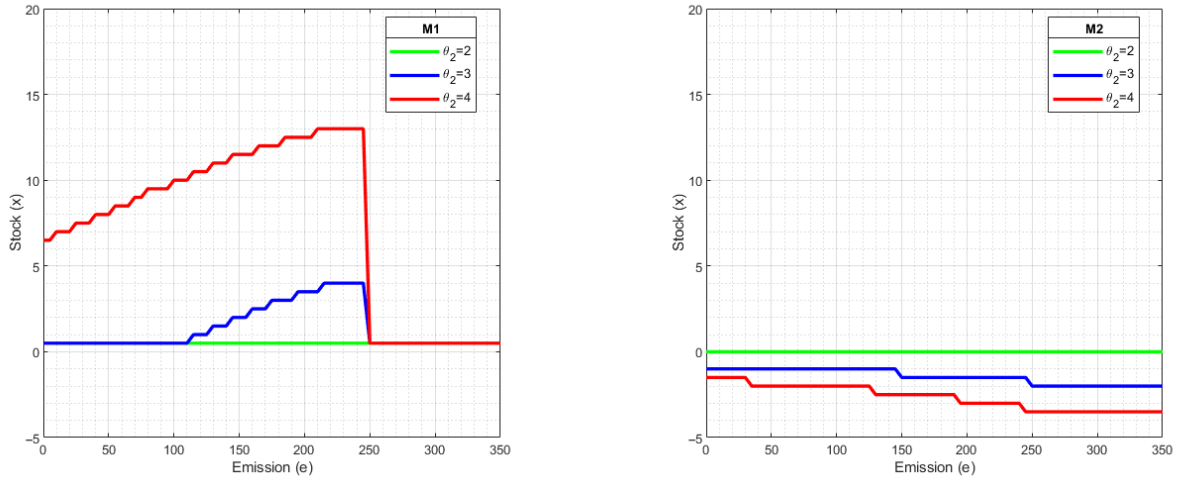

(**a**) Manufacturing machine (**b**) Remanufacturing machine

Figure 10. Variation in remanufacturing machine emission index and impact on critical thresholds.

6.6. Maximal Production Rates

Figure 11 examines the sensitivity of the optimal control policy to variations in the maximum manufacturing rate u_{1max}, considering values higher than those of the base case. When manufacturing capacity is sufficiently high, the manufacturing machine can satisfy demand on its own, thereby reducing the reliance on the remanufacturing machine to ensure service continuity. This increased flexibility allows the system to respond more effectively to stochastic capacity losses while maintaining inventory availability. Figure 12 complements this analysis by investigating the impact of changes in the maximum remanufacturing rate u_{2max}. The results highlight the supporting role of remanufacturing capacity in maintaining demand fulfillment when manufacturing resources are constrained, confirming the complementary nature of the two production modes in the hybrid system. The numerical results indicate that increasing the maximum production rate of either the manufacturing or the remanufacturing machine leads to a reduction in the corresponding critical inventory thresholds Z_1 and Z_3 as the emission level increases. Higher production capacities enable larger quantities of finished products to be generated over shorter time intervals, which accelerates the accumulation of GHG emissions. In response, the optimal policy adapts by lowering target inventory levels in order to limit emission-related penalties while preserving an economically efficient balance between production intensity and environmental compliance.

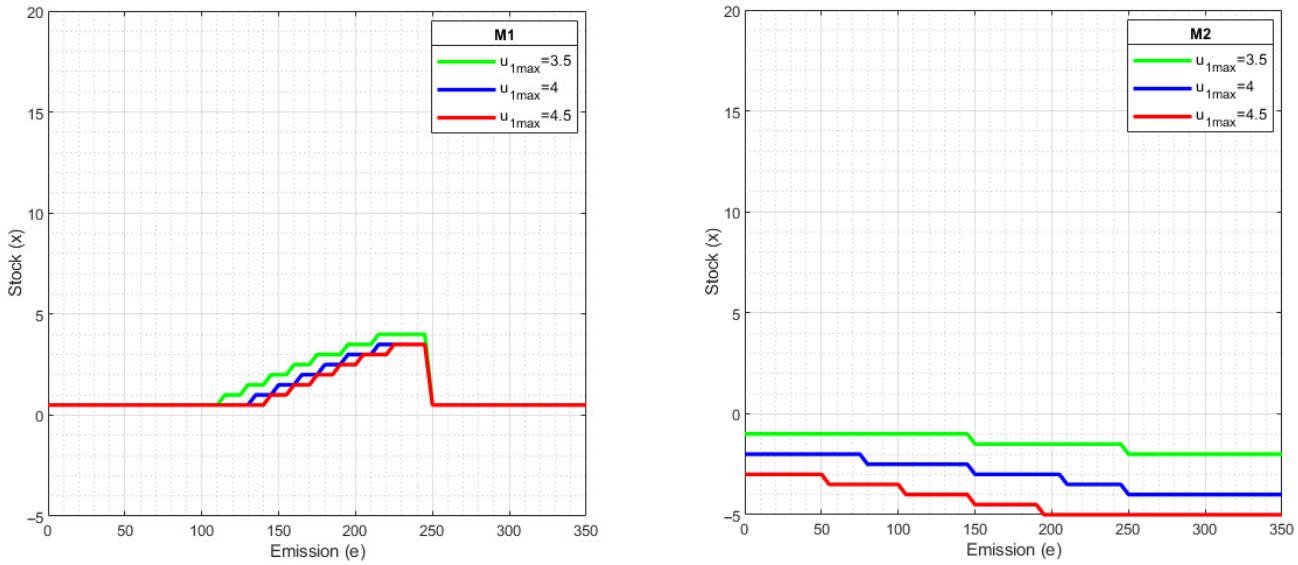

(**a**) Manufacturing machine (**b**) Remanufacturing machine

Figure 11. Variation in maximal manufacturing rate and impact on critical thresholds (high maximum production rates).

The numerical results indicate that increasing the maximum production rate of either the manufacturing or the remanufacturing machine leads to a reduction in the corresponding critical inventory thresholds Z_1 and Z_3 as the emission level increases. Higher production capacities allow larger quantities of finished products to be generated over shorter time intervals, which in turn accelerates the accumulation of GHG emissions. As a consequence, the optimal policy adapts by lowering the target inventory levels in order to limit emission-related penalties and maintain an economically efficient balance between production intensity and environmental compliance.

Overall, the sensitivity analysis confirms the structural stability of the proposed control policy with respect to variations in both economic and operational parameters. While the numerical values of the critical thresholds adjust in response to parameter changes, the

qualitative structure of the policy remains unchanged. The following section illustrates how these results can be translated into an implementation diagram that supports the practical application of the proposed control policy.

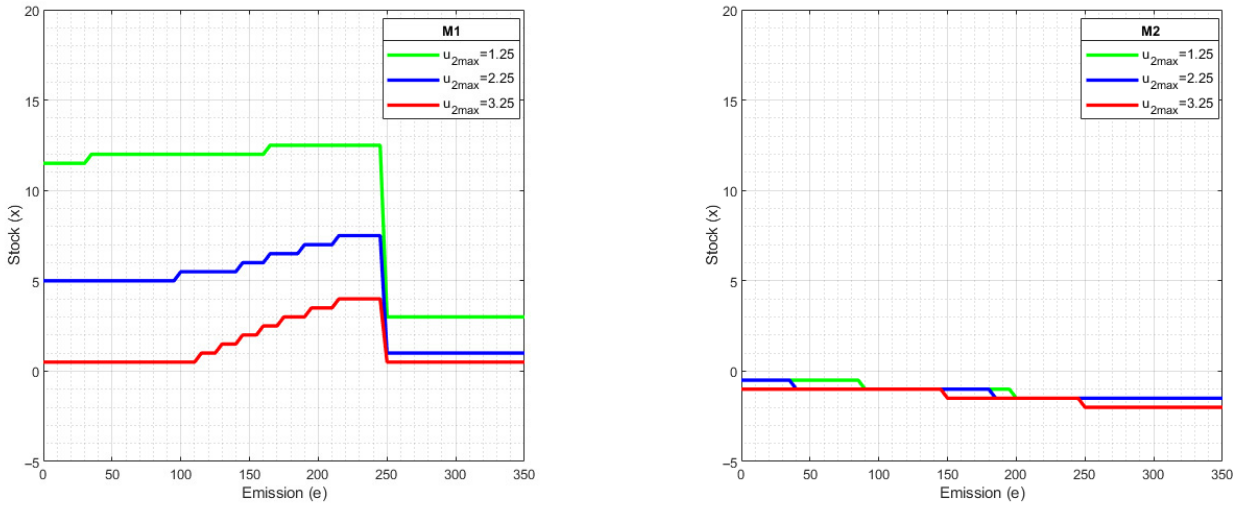

(**a**) Manufacturing machine (**b**) Remanufacturing machine

Figure 12. Variation in maximal remanufacturing rate and impact on critical thresholds.

7. Managerial Implications

The practical implementation of the proposed control policy requires continuous access to reliable information describing the state of the HMRS. In particular, decision-makers must be able to monitor the inventory level of serviceable products x, the cumulative greenhouse gas emission level e, and the operational status of both the manufacturing and remanufacturing machines. Such information can be obtained through modern production monitoring infrastructures that enable the systematic collection and consolidation of production, inventory, and environmental indicators.

From an operational perspective, the proposed policy provides a structured and actionable framework supporting managerial decision-making under both capacity disruptions and emission constraints. As illustrated in Figure 13, manufacturing and remanufacturing decisions are governed by the position of the inventory level x relative to emission-dependent critical thresholds (see Equations (24)–(27)). These thresholds define safety stock levels that protect the system against future machine failures and repair periods while accounting for the accumulation of emissions. When the inventory level falls below the relevant threshold, the policy prescribes increasing the manufacturing or remanufacturing rate in order to rebuild the buffer and reduce the risk of shortages. Conversely, when the inventory level exceeds the threshold, production activity is moderated or temporarily suspended to limit holding costs and avoid unnecessary emission accumulation.

The explicit consideration of the cumulative emission level e introduces an additional dimension to production control. As long as emissions remain below the regulatory limit L (i.e., $e < L$), the control policy favors inventory protection by maintaining relatively higher safety stock thresholds. When emissions approach or exceed the limit (i.e., $e \geq L$), the control policy progressively tightens production decisions by lowering the admissible inventory thresholds. This mechanism allows managers to adapt production intensity in response to environmental constraints while maintaining service continuity, rather than relying on rigid or static emission-control rules.

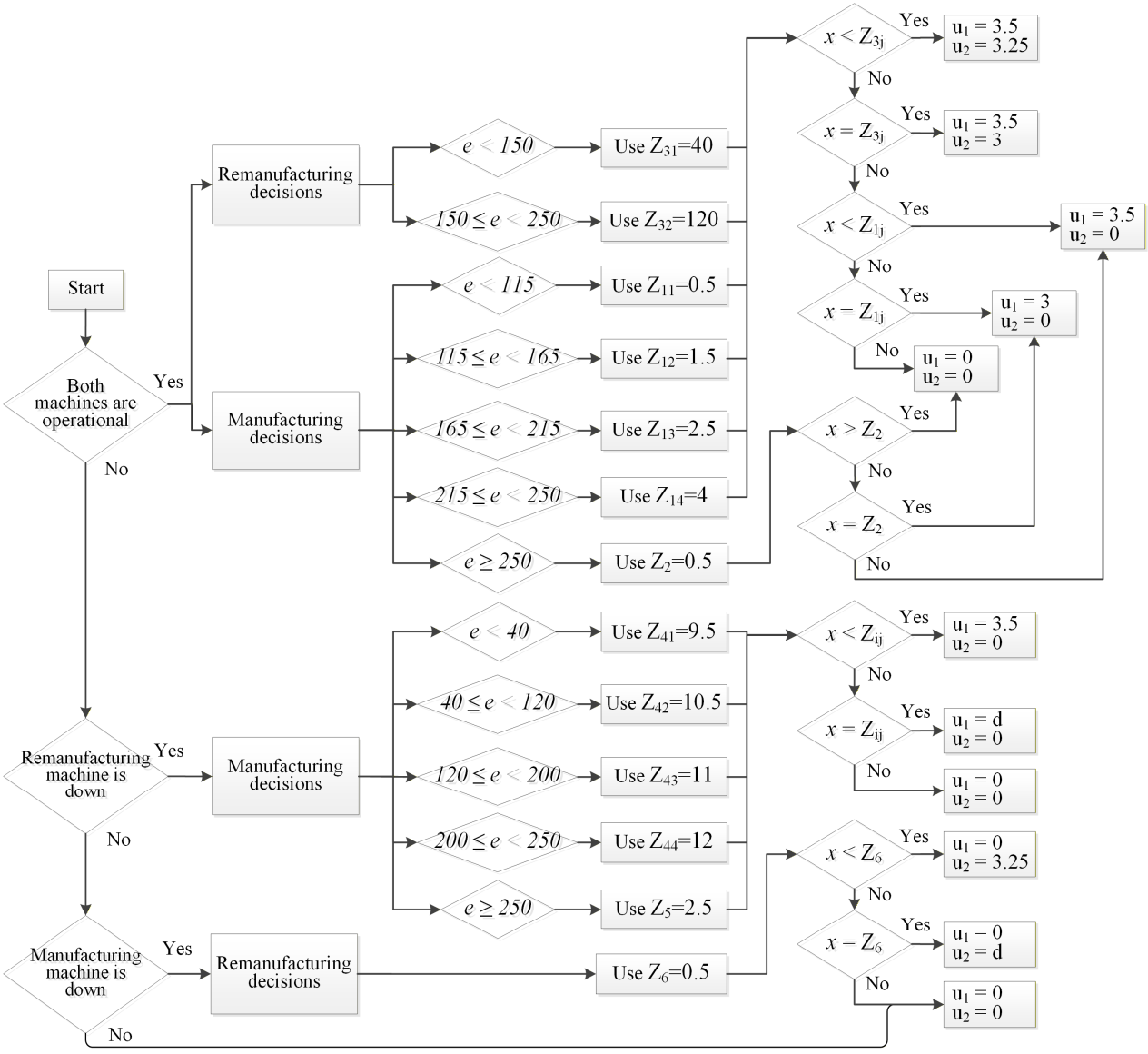

Figure 13. Implementation diagram of the control policy for the hybrid system.

Although the optimal control policy is originally defined through emission-dependent and state-contingent thresholds, its practical implementation does not require solving the stochastic optimization problem during system operation. The numerical analysis shows that the structure of the optimal policy, initially expressed through the control parameters Z_1, Z_2, Z_3, Z_4, Z_5, and Z_6, can be accurately captured by a limited number of representative threshold values. These values discretize the emission domain into a finite set of operational regions, within which production decisions follow clearly specified rules, namely production at maximum capacity, production at the demand rate, or production stoppage. This reduced representation preserves the essential structural properties of the optimal policy while significantly facilitating its operational deployment. The approximation was obtained through offline numerical experiments aimed at identifying a reduced set of threshold values that closely reproduce the behavior of the optimal solution. Figure 13 illustrates the resulting implementation logic of the proposed control policy, based on this finite set of emission and inventory thresholds. The corresponding parameter values used to delineate the operational regions are summarized as follows: $E_{11} = 115$, $E_{12} = 165$, $E_{13} = 115$, $E_2 = 70$, $E_{31} = 40$, $E_{32} = 120$, $E_{33} = 200$, $L = 250$, $Z_{11} = 0.5$, $Z_{12} = 1.5$, $Z_{13} = 2.5$, $Z_{14} = 4$, $Z_2 = 0.5$, $Z_{31} = -1$, $Z_{32} = -2$, $Z_{41} = 9.5$, $Z_{42} = 10.5$, $Z_{42} = 11$,

$Z_{44} = 12$, $Z_5 = 2.5$, and $Z_6 = 0.5$. These values provide managers with concrete reference points for adjusting manufacturing and remanufacturing rates according to the observed inventory level and cumulative emissions.

The proposed control framework equips managers with a robust and operationally meaningful decision-support tool for coordinating manufacturing and remanufacturing activities under stochastic disruptions and environmental regulation. By relying on predefined thresholds linked to inventory and emission states, decision-makers can respond effectively to changes in system conditions while limiting the risks of excessive emissions, inventory shortages, and penalty costs.

8. Conclusions and Discussion

This paper addressed the stochastic optimal control of a closed-loop HMRS operating under random machine failures and explicit GHG emission constraints. The system considered integrates two dedicated production resources, one for manufacturing and one for remanufacturing, whose availability is subject to stochastic breakdowns and repairs. The objective was to determine how manufacturing and remanufacturing rates should be jointly regulated over an infinite planning horizon in order to minimize the long-run expected total cost while ensuring compliance with environmental regulations. To tackle this problem, a stochastic dynamic programming framework was developed, enabling the coupled dynamics of inventory levels, machine availability, and cumulative emissions to be captured within a unified modeling approach. Since closed-form solutions are not available for such hybrid and failure-prone systems, the resulting optimality conditions were solved numerically using a finite-difference approximation scheme, allowing the structure of the optimal control policy to be characterized.

The numerical results showed that the optimal policy is governed by emission-dependent inventory thresholds that jointly regulate manufacturing and remanufacturing decisions. These thresholds control the formation and depletion of safety stock in response to stochastic capacity losses and emission accumulation. The resulting control policy adjusts production rates in a state-dependent manner to balance inventory-related costs, shortage risks, and emission penalties. Sensitivity analyses confirmed the robustness of the control policy structure with respect to variations in key system parameters, including failure and repair rates, emission limits, and cost coefficients, highlighting the consistency of the proposed framework across a wide range of operating conditions.

From an operational perspective, the proposed policy provides practical guidance for decision-makers managing HMRSs under environmental regulation. By linking production decisions to both the inventory state x and the cumulative emission level e relative to the regulatory limit L, the policy enables firms to mitigate the impact of random machine failures while limiting excessive emission penalties. The numerical results further indicated that the optimal policy can be implemented through a reduced set of representative thresholds that preserve the essential structure of the optimal solution while facilitating practical deployment. This feature enhances the relevance of the proposed framework for industrial applications where decision simplicity and robustness are critical.

From a broader perspective, this work contributes to the literature on sustainable operations by developing an integrated stochastic control framework for environmentally constrained HMRSs with unreliable resources. The model is motivated by operational challenges documented in remanufacturing sectors operating under environmental regulation and subject to stochastic production disruptions. By explicitly embedding cumulative emissions into production control decisions and deriving emission-dependent threshold policies, the proposed framework provides structured decision rules linking inventory dynamics, machine availability, and environmental compliance. The numerical experi-

ments presented in this study illustrate the structural behavior of the proposed policies under parameter configurations grounded in the remanufacturing and closed-loop supply chain literature. In addition, the computational framework used to solve the discretized HJB equations can be applied to different parameter values and system configurations when operational data become available. These characteristics support the relevance of the proposed approach for industrial decision-making contexts aligned with the objectives of Sustainability in Industry 4.0.

A key modeling assumption concerns the representation of reliability, emission dynamics, and environmental regulation. Machine state transitions are modeled as a continuous-time Markov process, implying exponentially distributed failure and repair times, while cumulative emissions are assumed to be linearly proportional to production rates and regulated through a cap-and-penalty mechanism activated when emissions exceed a prescribed limit. These assumptions ensure analytical tractability within the stochastic control framework and enable a clear characterization of the optimal threshold structure. However, real production systems may exhibit age-dependent or non-exponential failure behaviors, nonlinear emission patterns arising from operational conditions, and alternative regulatory instruments such as carbon taxes or emission trading schemes. Unlike the cap-based penalty considered here, a carbon tax would introduce continuously proportional emission costs, potentially leading to smoother adjustments of production thresholds, whereas emission trading schemes would add market-based price uncertainty to the decision process. Evaluating the impact of such non-Markovian reliability processes, nonlinear emission dynamics, and alternative environmental policy instruments on the structural properties of the proposed control policy represents a relevant extension of the present work. In addition, the present formulation considers two dedicated machines (manufacturing and remanufacturing), which allows for a clear analytical characterization of the hybrid system while maintaining a tractable state space. Extending the framework to systems with multiple parallel or heterogeneous machines would increase the dimensionality of the Markov state process and significantly enlarge the associated HJB system. Although the proposed stochastic control methodology remains applicable in principle to larger continuous-time Markov chain systems, such extensions would require advanced numerical schemes or approximation methods to mitigate the curse of dimensionality.

Several directions for future research can also be envisaged. The model could be extended to incorporate progressive system deterioration, more detailed reliability mechanisms, and stochastic customer demand and uncertain return flows in order to better reflect industrial operating conditions. Integrating maintenance decisions, including preventive or predictive maintenance, would enable a deeper analysis of the interactions between reliability, emissions, and production planning. Finally, extensions to multi-product or multi-stage HMRSs would further enhance the applicability of the proposed framework. Another potential extension involves applying the proposed framework to a fully documented industrial case study in order to empirically validate the emission-dependent threshold structure and quantify its operational and environmental benefits using real production data.

Author Contributions: All authors contributed to the study conception and modeling. Development of optimality conditions, data collection and simulation were performed by M.A., A.G., J.-P.K. and A.L.K.T. The first draft of the manuscript was written by M.A., and A.L.K.T. M.A., A.G. and J.-P.K. worked on the subsequent versions until the final version. The final manuscript was read and approved by M.A., A.G. and J.-P.K. All authors have read and agreed to the published version of the manuscript.

Funding: This research was supported by the Natural Sciences and Engineering Research Council of Canada (NSERC) under grant numbers RGPIN 2018-05292 and RGPIN-2020-05826.

Institutional Review Board Statement: Not applicable.

Informed Consent Statement: Not applicable.

Data Availability Statement: All data used in this study are presented in the manuscript. Further inquiries can be directed to the corresponding author.

Conflicts of Interest: The authors declare no conflicts of interest.

References

1. Filonchyk, M.; Peterson, M.P.; Yan, H.; Gusev, A.; Zhang, L.; He, Y.; Yang, S. Greenhouse gas emissions and reduction strategies for the world's largest greenhouse gas emitters. *Sci. Total Environ.* **2024**, *944*, 173895. [CrossRef]
2. Aragòn-Correa, J.A.; Marcus, A.A.; Vogel, D. The Effects of Mandatory and Voluntary Regulatory Pressures on Firms' Environmental Strategies: A Review and Recommendations for Future Research. *Acad. Manag. Ann.* **2020**, *14*, 339–365. [CrossRef]
3. Wu, D.; Li, K.; Cheng, Y. Green Investment and Emission Reduction in Supply Chains Under Dual-Carbon Regulation: A Dynamic Game Perspective on Coordination Mechanisms and Policy Insights. *Sustainability* **2025**, *17*, 8951. [CrossRef]
4. Wang, S.; Wan, L.; Li, T.; Luo, B.; Wang, C. Exploring the effect of cap-and-trade mechanism on firm's production planning and emission reduction strategy. *J. Clean. Prod.* **2018**, *172*, 591–601. [CrossRef]
5. Sajadi, S.M.; Behnamfar, R.; Sadeghi, M.; Tootoonchy, M. AI-enhanced simulation for sustainable production in pulp and paper industry. *Ann. Oper. Res.* **2026**. [CrossRef]
6. Butt, A.S.; Ali, I.; Govindan, K. The role of reverse logistics in a circular economy for achieving sustainable development goals: A multiple case study of retail firms. *Prod. Plan. Control* **2024**, *35*, 1490–1502. [CrossRef]
7. Paul, M.; Reinhart, G. Towards the integration of remanufacturing into existing manufacturing systems. *Procedia CIRP* **2024**, *130*, 1447–1453. [CrossRef]
8. Li, J.; Lai, K.K.; Li, Y. Remanufacturing and low-carbon investment strategies in a closed-loop supply chain under multiple carbon policies. *Int. J. Logist. Res. Appl.* **2024**, *27*, 170–192. [CrossRef]
9. Gershwin, S.B. The future of manufacturing systems engineering. *Int. J. Prod. Res.* **2018**, *56*, 224–237. [CrossRef]
10. Lozano-Oviedo, J.; Cortés, C.E.; Rey, P.A. Sustainable closed-loop supply chains and their optimization models: A review of the literature. *Clean Technol. Environ. Policy* **2024**, *26*, 999–1023. [CrossRef]
11. Rizova, M.I.; Wong, T.C.; Ijomah, W. A systematic review of decision-making in remanufacturing. *Comput. Ind. Eng.* **2020**, *147*, 106681. [CrossRef]
12. Van Der Laan, E.; Salomon, M.; Dekker, R. An Investigation of lead-time effects in manufacturing/remanufacturing systems under simple PUSH and PULL control strategies. *Eur. J. Oper. Res.* **1999**, *115*, 195–214. [CrossRef]
13. Dobos, I. Optimal production-inventory strategies for a HMMS-type reverse logistics system. *Int. J. Prod. Econ.* **2003**, *81–82*, 351–360. [CrossRef]
14. Gayon, J.P.; Vercraene, S.; Flapper, S.D.P. Optimal control of a production-inventory system with product returns and two disposal options. *Eur. J. Oper. Res.* **2017**, *262*, 499–508. [CrossRef]
15. Aminipour, A.; Bahroun, Z.; Hariga, M. Cyclic manufacturing and remanufacturing in a closed-loop supply chain. *Sustain. Prod. Consum.* **2021**, *25*, 43–59. [CrossRef]
16. Cheng, Z. Stochastic dynamic production planning in hybrid manufacturing and remanufacturing system with random usage durations. *Int. J. Prod. Res.* **2024**, *62*, 2331–2349. [CrossRef]
17. Akella, R.; Kumar, P. Optimal control of production rate in a failure prone manufacturing system. *IEEE Trans. Autom. Control* **1986**, *31*, 116–126.
18. Korugan, A.; Dingeç, K.D.; Önen, T.; Ateş, N.Y. On the quality variation impact of returns in remanufacturing. *Comput. Ind. Eng.* **2013**, *64*, 929–936. [CrossRef]
19. Turki, S.; Didukh, S.; Sauvey, C.; Rezg, N. Optimization and Analysis of a Manufacturing–Remanufacturing–Transport–Warehousing System within a Closed-Loop Supply Chain. *Sustainability* **2017**, *9*, 561. [CrossRef]
20. Koulinas, G.K.; Paraschos, P.D.; Koulouriotis, D.E. A machine learning framework for explainable knowledge mining and production, maintenance, and quality control optimization in flexible circular manufacturing systems. *Flex. Serv. Manuf. J.* **2024**, *36*, 737–759. [CrossRef]
21. Assid, M.; Gharbi, A.; Hajji, A.; Pellerin, R. Coordinated production and opportunistic-preventive maintenance control policy in deteriorating hybrid manufacturing–remanufacturing systems. *Flex. Serv. Manuf. J.* **2025**. [CrossRef]
22. Bazan, E.; Jaber, M.Y.; Zanoni, S. Carbon emissions and energy effects on a two-level manufacturer-retailer closed-loop supply chain model with remanufacturing subject to different coordination mechanisms. *Int. J. Prod. Econ.* **2017**, *183*, 394–408. [CrossRef]
23. Wang, X.; Han, S. Optimal operation and subsidies/penalties strategies of a multi-period hybrid system with uncertain return under cap-and-trade policy. *Comput. Ind. Eng.* **2020**, *150*, 106892. [CrossRef]

24. Shekarian, E.; Marandi, A.; Majava, J. Dual-channel remanufacturing closed-loop supply chains under carbon footprint and collection competition. *Sustain. Prod. Consum.* **2021**, *28*, 1050–1075. [CrossRef]
25. Jauhari, W.A.; Pujawan, I.N.; Suef, M. A closed-loop supply chain inventory model with stochastic demand, hybrid production, carbon emissions, and take-back incentives. *J. Clean. Prod.* **2021**, *320*, 128835. [CrossRef]
26. Lahmar, H.; Dahane, M.; Mouss, K.N.; Haoues, M. Multi-objective sustainable production planning for a hybrid multi-stage manufacturing-remanufacturing system with grade-based classification of recovered and remanufactured products. *J. Intell. Manuf.* **2025**, *36*, 1385–1407. [CrossRef]
27. Kenné, J.-P.; Gharbi, A.; Takengny, A.L.K.; Assid, M. Optimal Control Policy of Unreliable Production Systems Generating Greenhouse Gas Emission. *Sustainability* **2024**, *16*, 5760. [CrossRef]
28. Ndhaief, N.; Nidhal, R.; Hajji, A.; Bistorin, O. Environmental issue in an integrated production and maintenance control of unreliable manufacturing/remanufacturing systems. *Int. J. Prod. Res.* **2020**, *58*, 4182–4200. [CrossRef]
29. Merghem, M.; Haoues, M.; Senoussi, A.; Dahane, M.; Mouss, N.K. Integrated production and maintenance planning in imperfect hybrid manufacturing–remanufacturing systems with outsourcing and carbon emissions. *Int. J. Prod. Econ.* **2026**, *291*, 109862. [CrossRef]
30. Liu, Y.; Liu, B.; Yang, H.; Luo, K. Optimal production and maintenance strategies for manufacturing/remanufacturing leasing system considering uncertain quality and carbon emission. *Int. J. Prod. Econ.* **2025**, *280*, 109489. [CrossRef]
31. Gharbi, A.; Kenné, J.-P.; Takengny, A.L.K.; Assid, M. Joint Emission-Dependent Optimal Production and Preventive Maintenance Policies of a Deteriorating Manufacturing System. *Sustainability* **2024**, *16*, 6146. [CrossRef]
32. Kushner, H.J.; Dupuis, P.G. *Numerical Methods for Stochastic Control Problems in Continuous Time*; Springer Nature: New York, NY, USA, 1992.
33. Ferguson, M. Strategic issues in closed-loop supply chains with remanufacturing. In *Closed-Loop Supply Chains: New Developments to Improve the Sustainability of Business Practices*; Auerbach Publications: New York, NY, USA, 2010; pp. 9–21.
34. Wang, W.; Mo, D.Y.; Wang, Y.; Tseng, M.M. Assessing the cost structure of component reuse in a product family for remanufacturing. *J. Intell. Manuf.* **2019**, *30*, 575–587. [CrossRef]
35. Dominguez, R.; Cannella, S.; Ponte, B.; Framinan, J.M. On the dynamics of closed-loop supply chains under remanufacturing lead time variability. *Omega* **2020**, *97*, 102106. [CrossRef]
36. Zhou, J.; Deng, Q.; Li, T. Optimal acquisition and remanufacturing policies considering the effect of quality uncertainty on carbon emissions. *J. Clean. Prod.* **2018**, *186*, 180–190. [CrossRef]
37. Chen, C.; Monahan, G.E. Environmental safety stock: The impacts of regulatory and voluntary control policies on production planning, inventory control, and environmental performance. *Eur. J. Oper. Res.* **2010**, *207*, 1280–1292. [CrossRef]
38. Sundin, E.; Lee, H.M. In what way is remanufacturing good for the environment? In *Design for Innovative Value Towards a Sustainable Society*; Springer: Dordrecht, The Netherlands, 2012; pp. 552–557. [CrossRef]
39. Bazan, E.; Jaber, M.Y.; El Saadany, A.M.A. Carbon emissions and energy effects on manufacturing-remanufacturing inventory models. *Comput. Ind. Eng.* **2015**, *88*, 307–316. [CrossRef]